FULL PAPER

Dalton
www.rsc.org/dalton

Immobilisation of electroactive macrocyclic complexes within titania films

Paul V. Bernhardt,*[a] Nathan L. Kilah,[a] Andrew P. Meacham,[a] Paul Meredith[b] and Robert Vogel[b]

[a] *Department of Chemistry, University of Queensland, Brisbane 4072, Australia*
[b] *School of Physical Sciences, University of Queensland, Brisbane 4072, Australia*

Received 27th April 2005, Accepted 20th June 2005
First published as an Advance Article on the web 1st July 2005

The 4-carboxyphenyl-appended macrocyclic ligand *trans*-6,13-dimethyl-6-((4-carboxybenzyl)amino)-1,4,8,11-tetraazacyclotetradecane-6-amine (HL^{10}) has been synthesised and complexed with Co^{III}. The mononuclear complexes $[Co(HL^{10})(CN)]^{2+}$ and $[CoL^{10}(OH)]^{+}$ have been prepared and the crystal structures of their perchlorate salts are presented, where the ligand is bound in a pentadentate mode in each case while the 4-carboxybenzyl-substituted pendent amine remains free from the metal. The cyano-bridged dinuclear complex $[CoL^{10}$-μ-NC-$Fe(CN)_5]^{2-}$ was also prepared and chemisorbed on titania-coated ITO conducting glass. The adsorbed complex is electrochemically active and cyclic voltammetry of the modified ITO working electrode in both water and MeCN solution was undertaken with simultaneous optical spectroscopy. This experiment demonstrates that reversible electrochemical oxidation of the Fe^{II} centre is coupled with rapid changes in the optical absorbance of the film.

Introduction

Macromonocyclic tetraamines bearing potentially coordinating appended functional groups (pendent arms) represent a versatile class of multidentate ligand. Substituents attached either to the ring N-donors or the C-atom framework expand the coordinating ability of the ligand from typically tri- or tetradentate to penta- and hexadentate thus enabling the partial or complete encapsulation of octahedral metal ions. Primary amines and carboxylic acids are the more common examples of pendent arms that have been introduced to the macrocyclic periphery. Although functionalisation of the ring secondary amines is a direct route to N-functionalised macrocycles, selectivity is an issue, with partial protection of the N-donors being necessary unless complete alkylation is desired. An additional drawback with this approach is that the ensuing sterically crowded tertiary amines are poorer ligands than their secondary amine precursors and this can lead to complications such as slow complexation kinetics, mixtures of N-based isomers and lower formation constants.

Our efforts in the area of functionalised macrocyclic chemistry have focussed exclusively on attaching substituents to the C-atom framework[1] by using ligands such as the hexamine L^1 (in this case in its *trans* isomeric form) or the pentaamine analogue L^2 (Chart). Both of these ligands are easily synthesised in large quantities.[2–4] The exocyclic amines in these ligands may serve two purposes. With respect to metal ion complexation, the primary amines of L^1 and L^2 expand the coordinating ability of the ligand to hexadentate or pentadentate, respectively, relative to the tetradentate mode of an unsubstituted cyclam ligand. On the other hand, these exocyclic primary amines are ideal targets for the attachment of redox active centres (ferrocene, L^3),[5] fluorophores (anthracene, L^8)[6] and metal binding groups (crown ethers, L^9)[7] as shown in the Chart. In studies to date, we have found[7–10] that functionalisation of the exocyclic amines renders them incapable of coordination, presumably due to steric effects. That is, ligands such as L^9 behave effectively as pentadentates when complexed with octahedral metal ions (in the same way as L^2), with the four macrocyclic secondary amines plus the exocyclic primary amine coordinated.

An earlier investigation of this chemistry involved the attachment of both aromatic and aliphatic carboxylic acids to the mono-amino-substituted cyclam L^2.[9] The Cu^{II} complexes of the carboxylic acid functionalised ligands L^5–L^7 were sufficiently reactive that they could be coupled with surface lysine residues on the protein bovine serum albumin to afford the corresponding Cu-labelled proteins.

Carboxylic acids also exhibit a high affinity for metal oxides. Here we have turned our attention to the grafting of macrocyclic Co^{III} complexes onto nanocrystalline TiO_2 using the new benzoic acid functionalised macrocycle L^{10}. Titania exists in three phases; rutile, brookite (which rapidly converts to rutile at low temperatures) and the semiconductor anatase.[11] On the surface of titania there are Ti atoms that require additional O-atoms to complete their preferred coordination sphere. Oxygen-containing functional groups such as carboxylic acids are strongly chemisorbed and the result is a new Ti–OCOR bond.[12,13] The binding mode *e.g.* mono-, bidentate, bridging *etc.*, varies with the temperature of chemisorption as indicated by FT-IR spectroscopy through a decrease in the asymmetric $\bar{\nu}_{OCO}$ stretching band for the monodentate coordinated acid and a subsequent increase in the degree of bidentate coordination above 100 °C.[14,15]

Nanostructured anatase may be supported on a conducting glass substrate and incorporated into an electrical circuit for a variety of applications. Dye-sensitised photoelectrochemical cells comprising Ru polypyridine dyes as the sensitiser anchored to titania were first reported by Grätzel and co-workers[16] and this has been a very active area of research over the last 20 or so years. The Ru dyes are attached to TiO_2 through carboxylic acid functional groups appended to the polypyridine ligand thus ensuring high quantum efficiency for photoelectron injection into the conduction band of titania and then into the electrical circuit of the device. A similar principle has been applied by Bignozzi *et al.* in the covalent attachment of photoactive and electrochromic transition metal containing dyes to TiO_2 *via* functional groups such as phosphonic, boronic and carboxylic acids.[17–19] Inclusion of acid functionality has facilitated the chemisorption of electrochromic viologen dyes to the surface of titania.[20–23] Both photoelectrochemical and electrochromic applications require the formation of optically transparent films of the dye in addition to effective electronic communication between the dye and the conducting surface, which is usually conducting glass *e.g.* indium-doped SnO_2 applied as a thin film onto a glass slide. Here we demonstrate that macrocyclic ligands such as L^{10} provide an ideal scaffold for the covalent attachment of tightly bound transition metal ions onto titania.

DOI: 10.1039/b505917h

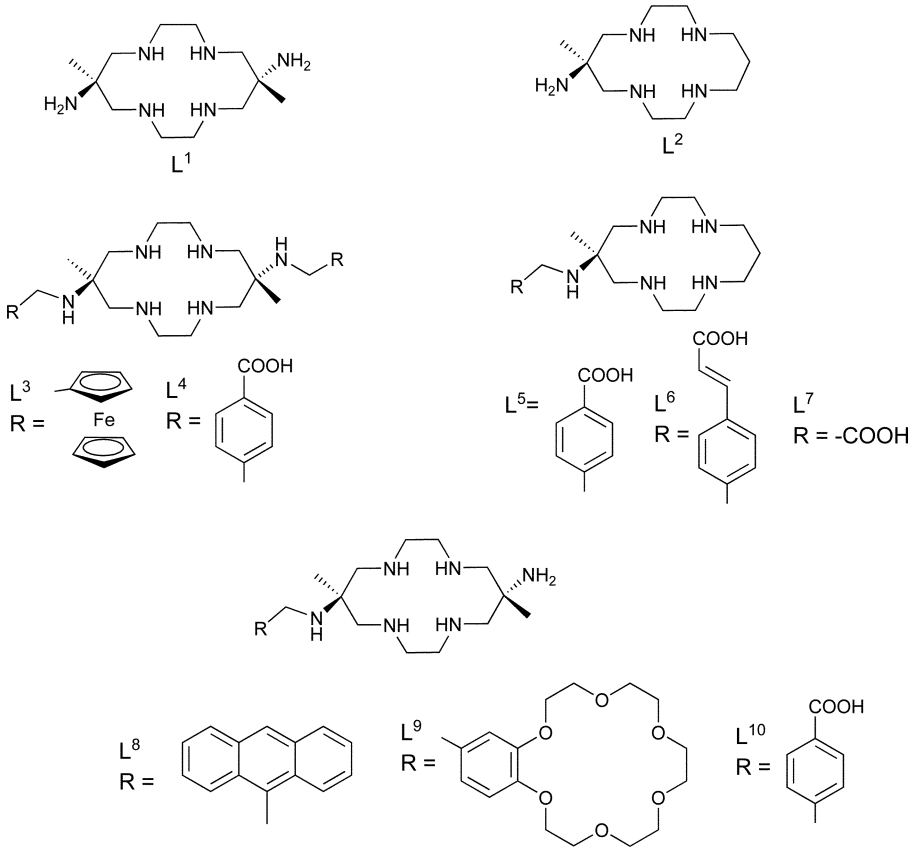

Chart 1

Experimental

Safety note

The release of HCN gas requires carefully controlled conditions allowing adequate ventilation to avoid inhalation and personal protective equipment to prevent absorption through the skin. Perchlorate salts are potentially explosive and should only be handled in small quantities and should never be heated in the solid state or scraped from a sintered glass frit.

Syntheses

The parent ligand *trans*-6,13-dimethyl-1,4,8,11-tetraazacyclotetradecane-6,13-diamine (L^1) was prepared as described.[24] $Na_3[Co(CO_3)_3]\cdot 3H_2O$ was synthesised according to a published procedure.[25]

(a) Synthesis of crude ligand HL^{10}. In a well ventilated fume hood, $L^1\cdot 6HCl$ (4.77 g, 10 mmol) was dissolved in EtOH : H_2O (300 cm^3, 9 : 1 *v*/*v*) by raising the apparent pH to 5.5 with sodium hydroxide solution. Sodium cyanoborohydride (1.88 g, 30 mmol) was added and the pH readjusted to 5.5 (*caution!*). 4-Carboxybenzaldehyde (1.50 g, 10 mmol) was added with stirring and the pH was maintained at 5.5 for 3 h through the periodic addition of dil. HCl. The reaction mixture was left to stir overnight, resulting in a mixture of L^4, L^{10} and 4-hydroxymethylbenzoic acid which coprecipitated as their sodium/hydrogen salt. Purification of this mixture was carried out by complexation and column chromatography as described below.

(b) $[Co(HL^{10})(CN)](ClO_4)_2$. The suspension from part (a) was evaporated to dryness (*caution!*—contains residual cyanide) then resuspended in water (400 cm^3) in a fume hood. The pH was raised to 8 and $Na_3[Co(CO_3)_3]\cdot 3H_2O$ (3.62 g, 10 mmol) was added with stirring. This mixture was heated to *ca.* 60 °C and left to stir overnight. A black precipitate of cobalt oxide was filtered off and the solution was diluted to 10 dm^3 and loaded onto a Sephadex C-25 cation exchange column (60 cm × 3.5 cm, Na^+ form). Four distinct bands were obtained in the order given below using various concentrations of aqueous $NaClO_4$ solution as eluent. All compounds were isolated as perchlorate salts (*caution!*) by concentrating the eluate to small volume (*ca.* 40 cm^3) which afforded crystals upon standing at room temperature.

Band 1 (0.05 mol dm^{-3} $NaClO_4$, pale yellow, minor): *trans*-$[CoL^1(CN)_2]ClO_4$ (λ_{max} 411 nm).

Band 2 (0.05 mol dm^{-3} $NaClO_4$, yellow, major): *trans*-$[CoL^{10}(CN)](ClO_4)_2$ (λ_{max} 430 nm). The eluate pH was adjusted to 3 resulting in precipitation of X-ray quality crystals of $[Co(HL^{10})(CN)](ClO_4)_2\cdot H_2O$. Anal. Found: C, 35.68; H, 5.51; N, 13.86 Calc. for $CoC_{21}H_{36}N_7Cl_2O_{10}\cdot 2H_2O$: C, 35.40; H, 5.66; N, 13.76. Electronic spectrum (H_2O): λ_{max}/nm (ε/dm^3 mol^{-1} cm^{-1}) 430 (87). ^1H NMR (D_2O-TSP) 1.14 (s, 3H, CH_3), 1.24 (s, 3H, CH_3), 2.15–3.59 (m, 16H, macrocyclic CH_2) 3.77 (s, 2H CH_2), 7.59, 7.68 (q, 4H, *p*-substitution). ^{13}C NMR (D_2O-TSP) 20.97, 23.64, 47.63, 54.09, 55.41, 58.87, 60.24, 62.88, 66.83, 72.46, 131.30, 132.27, 138.23 147.05, 178.02.

Band 3 (0.2 mol dm^{-3} $NaClO_4$, yellow, minor): *trans*-$[CoL^1(CN)](ClO_4)_2$ (λ_{max} 434 nm).

Band 4 (0.5 mol dm^{-3} $NaClO_4$, yellow, minor): $[CoL^1](ClO_4)_3$ (λ_{max} 326, 447 nm).

The compounds isolated from bands 1 and 3 are reported elsewhere[26] and the compound from band 4 has also been characterised previously.[2]

(c) *trans*-$[CoL^{10}(OH)]ClO_4\cdot 5H_2O$. In a well ventilated fume hood, the crude reaction mixture from part (a) was acidified with HCl (1 mol dm^{-3}) to pH 3 with stirring and then aerated vigorously to purge the solution of HCN gas (*caution!*). Additional aliquots of acid were added to maintain a pH of 3 and removal of HCN was judged to be complete when no further rise in pH was observed. $Na_3[Co(CO_3)_3]\cdot 3H_2O$ (3.62 g, 10 mmol) was added and the mixture was stirred at 60 °C overnight, filtered

and the filtrate was diluted to 10 dm^3. Sephadex C-25 column chromatography (as above) yielded four bands.

Band 1 (0.05 mol dm^{-3} $NaClO_4$, pale yellow, minor): *trans*-$[CoL^1(CN)_2]ClO_4$.

Band 2 (0.05 mol dm^{-3} $NaClO_4$, yellow, minor): *trans*-$[CoL^{10}(CN)](ClO_4)_2$.

Band 3 (0.2 mol dm^{-3} $NaClO_4$, orange, major): *trans*-$[CoL^{10}(OH_2)]^{2+}$. This desired fraction was concentrated to approximately 100 cm^3 and the pH was adjusted to 13 resulting in precipitation of X-ray quality crystals of $[CoL^{10}(OH)]ClO_4 \cdot 5H_2O$. NMR spectra were recorded of the more soluble aqua complex, generated *in situ* through the addition of trifluoroacetic acid. Anal. Found: C, 38.77; H, 6.75; N, 13.19 Calc. for $CoC_{20}H_{34}N_6ClO_7 \cdot 3H_2O$: C, 38.68; H, 6.82; N, 13.53. Electronic spectrum (H_2O): λ_{max}/nm (ε/dm^3 mol^{-1} cm^{-1}) 480 (105), 339 (163) ^{1}H NMR (D_2O-TSP) 1.14 (s, 3H, CH_3), 1.24 (s, 3H, CH_3), 2.15–3.59 (m, 16H, macrocyclic CH_2) 3.77 (s, 2H CH_2), 7.58, 7.60 (q, 4H, *p*-disubstituted phenyl). ^{13}C NMR (D_2O-TSP) 18.89, 22.33, 46.21, 53.57, 58.10, 58.44, 60.56, 67.62, 70.97, 129.86, 131.48, 146.52.

Band 4 (0.5 mol dm^{-3} $NaClO_4$, yellow, minor): $[CoL^1](ClO_4)_3$ (λ_{max} 326, 447 nm).

(d) $Na[Co^{III}(HL^{10})$-μ-NC-$Fe^{II}(CN)_5]\cdot 6H_2O$. *trans*-$[CoL^{10}(OH)]ClO_4 \cdot 5H_2O$ (0.6 g, 1.1 mmol) was dissolved in water (300 cm^3) at pH 7. $K_4[Fe(CN)_6]$ (0.4 g, 1.1 mmol) was added and the reaction mixture darkened after a few minutes. The solution was heated to 60 °C and left to stir overnight. pH was readjusted to 7 and the solution was diluted to approximately 10 dm^3. This solution was sorbed onto a Sephadex DEAE A-25 anion exchange (45 cm × 4 cm, ClO_4^- form) and eluted with $NaClO_4$.

Band 1 (red, 0.05 mol dm^{-3} $NaClO_4$) eluted rapidly and is most probably the neutral trinuclear complex $Co^{III}L^{10}$-μ-NC-$Fe^{II}(CN)_4$-μ-CN-$Co^{III}L^{10}$ but this was not present in sufficient quantity to enable its isolation as a solid.

Band 2 (red, 0.2 mol dm^{-3} $NaClO_4$). After concentration of this band to *ca.* 20 cm^3 EtOH was added to afford a co-precipitate of the complex and $NaClO_4$. This was recrystallised by vapour diffusion of MeOH into a concentrated aqueous solution of the crude product. Anal. Found: C, 39.25; H, 5.81; N, 21.08 Calc. for $C_{26}H_{36}CoFeN_{12}NaO_2 \cdot 6H_2O$ C, 39.31; H, 6.09; N, 21.16%. Electronic spectrum (H_2O): λ_{max}/nm (ε/dm^3 mol^{-1} cm^{-1}) 509 (585), 440 (451), 321 (504). ^{1}H NMR (D_2O-TSP) 1.26 (s, 3H, CH_3), 1.31 (s, 3H, CH_3), 2.17–3.72 (m, 16H, macrocyclic CH_2) 4.03 (s, 2H CH_2), 7.87, 8.07 (q, 4H, *p*-substituted). ^{13}C NMR (D_2O-TSP) 20.96, 23.47, 48.34, 54.55, 54.90, 59.27, 60.51, 62.05, 68.46, 72.41, 132.09, 132.80, 138.29, 177.66, 178.11, 180.84, 193.46. Infrared (KBr disc): $\bar{\nu}$/cm^{-1} 2048 (equatorial CN), 2069 (axial CN), 2117 (μ-CN).

(e) $[Co^{III}(HL^{10})$-μ-NC-$Fe^{III}(CN)_5]\cdot 9H_2O$. A *ca.* 50 cm^3 aliquot of band 2 directly from the chromatography column from the previous synthesis was treated with $K_2S_2O_8$ (0.1 g). The solution gradually changed from maroon to yellow over the period of a couple of hours. On standing, yellow microcrystals of the compound deposited which were filtered off and air dried. Anal. Found: C, 37.89; H, 5.99; N, 20.42. Calc. for $C_{26}H_{36}CoFeN_{12}O_2 \cdot 9H_2O$ C, 37.83; H, 6.59; N, 20.36%. Electronic spectrum (H_2O): λ_{max}/nm (ε/dm^3 mol^{-1} cm^{-1}) 435 (1550), 410 (sh, 1200), 320 (sh, 1800). Infrared (KBr disc): $\bar{\nu}$/cm^{-1} 2113 (equatorial CN), 2120 (axial CN), 2170 (μ-CN).

Preparation of P25 titania films

Titanium dioxide films were prepared through suspension of P25 colloidal titania particles (12 g) in a pH 3–4 solution of dil. nitric acid combined with 1 cm^3 of cetyltrimethylammonium chloride (CTAC) surfactant.[27] This suspension was ground with a mortar and pestle and finally stirred to a consistent paste. A thin layer of titanium dioxide was laid onto the conducting side of a transparent ITO electrode through a drag coating procedure derived from a literature method.[28] The film was left overnight to cure until dry and was then heated in a furnace. The temperature was increased at a rate of 1 min^{-1} to a temperature of 450 °C for removal of the surfactant and annealing of the P25 particles.

Chemisorption of $[Co(HL^{10})$-μ-NC-$Fe(CN)_5]^-$ on titania films

A P25 titanium oxide film on ITO prepared as above was heated in a furnace to 400 °C for 2 h and allowed to cool to 100 °C. Two different adsorption methods were found to be successful.

(i) Aqueous method: A *ca.* 500 μmol dm^{-3} solution of $[CoL^{10}$-μ-NC-$Fe(CN)_5]^{2-}$ in water was acidified to pH 3.5 with HCl solution (0.01 mol dm^{-3}) and the slide was placed in the solution whilst hot and allowed to soak overnight. The resulting film was removed from the solution, washed with methanol and air dried.

(ii) Nonaqueous method: A TiO_2 coated ITO glass slide was soaked in a 5 mmol dm^{-3} solution of $[CoL^{10}$-μ-NC-$Fe(CN)_5]^{2-}$ in MeOH : EtOH (1 : 1) overnight. The slide was removed from the solution and washed well with MeOH then EtOH.

Physical methods

Electronic spectra were recorded on a Perkin-Elmer Lambda 40 spectrophotometer and infrared spectra were recorded on a Perkin-Elmer 1600 Series FTIR spectrometer. NMR spectra were measured on a Bruker AC400 at 400 MHz for ^{1}H spectra and 100 MHz for ^{13}C spectra. Samples were measured as D_2O solutions and were referenced to the methyl resonance of sodium(trimethylsilyl)propionate. Electrochemical measurements were undertaken with a BAS100B/W potentiostat utilising a Pt wire counter and Ag/AgCl reference electrode (+196 mV *vs.* NHE). The working electrode was either glassy carbon (BAS C2 cell stand) or mercury drop working electrode (EG&G PARC Model 303 SMDE) or a small piece of optically transparent indium-doped tin oxide (ITO). Solutions contained approximately 1 mmol dm^{-3} analyte and 0.1 mol dm^{-3} $NaClO_4$ as supporting electrolyte in H_2O. X-ray photoelectron spectroscopy (XPS) data were acquired using a Kratos Axis ULTRA X-ray Photoelectron Spectrometer incorporating a 165 mm hemispherical electron energy analyser and utilising incident monochromatic Al X-rays (1486.6 eV) at 150 W (15 kV, 10 mA). Survey (wide) scans were taken at analyser pass energy of 160 eV and multiplex (narrow) high-resolution scans at 20 eV. Base pressure in the analysis chamber was 1.0×10^{-9} Torr and during sample analysis was of 10^{-8} Torr in magnitude.

Crystallography

Cell constants were determined by a least squares fit to the setting parameters of 25 independent reflections measured on an Enraf-Nonius CAD4 four-circle diffractometer employing graphite-monochromated Mo-Kα radiation (0.71073) and operating in the ω–2θ scan mode. Data reduction and empirical absorption corrections (ψ-scans)[29] were performed with the WINGX[30] package. Structures were solved and refined with the SHELX suite of programs.[31] All non hydrogen atoms with the exception of disordered perchlorate oxygen atoms were modelled with anisotropic thermal parameters. Hydrogen atoms were modelled for all water molecules where visible in the difference map. All other H atoms were included at estimated positions using a riding model. Drawings of all molecules were prepared with ORTEP3.[32]

Crystal data

$[Co(HL^{10})(CN)](ClO_4)_2\cdot H_2O$. $C_{21}H_{38}Cl_2CoN_7O_{11}$, M = 694.41, triclinic, space group $P\bar{1}$ (No. 2), a = 9.366(1), b = 13.012(2), c = 13.069(1) Å, α = 106.045(9), β = 105.90(1), γ = 93.07(1)°, U = 1457.6(3) Å^3, T = 293 K, Z = 2, μ(Mo-Kα) = 8.41 cm^{-1}, 5460 reflections measured, 5119 unique (R_{int} 0.0304)

which were used in all calculations, $R_1 = 0.0437$ (for 3890 obs. data, $I > 2\sigma(I)$), $wR_2 = 0.1258$ (all data).

[CoL^{10}(OH)]ClO$_4$·5H$_2$O. $C_{20}H_{46}ClCoN_6O_{12}$, $M = 657.01$ g. mol^{-1}, monoclinic, space group $P2_1/c$ (No. 14), $a = 9.235(3)$, $b = 24.023(3)$, $c = 13.845(2)$ Å, $\beta = 109.01(2)°$, $U = 2904(1)$ Å^3, $T = 293$ K, $Z = 4$, μ(Mo-Kα) = 7.51 cm^{-1}, 5441 reflections measured, 5105 unique (R_{int} 0.0292) which were used in all calculations, $R_1 = 0.0684$ (for 3606 obs. data, $I > 2\sigma(I)$), $wR_2 = 0.2381$ (all data).

CCDC reference numbers 270349 and 270350.

See http://dx.doi.org/10.1039/b505917h for crystallographic data in CIF or other electronic format.

Results and discussion

Synthesis

The parent ligand, L^1, is of great use in synthetic coordination chemistry due to the ease of direct functionalisation and also in the chemical stability of its transition metal complexes. Selective reductive alkylation is a particularly versatile procedure employing suitable aldehydes in reaction with the pendent amines, and this can be achieved through a combination of optimised pH conditions and appropriate reductants.[7,33]

The degree of substitution can be controlled through selective protonation of the pendent amine (pK_a values of 5.5 and 6.3).[34] The first five stepwise protonation constants of L^1 (expressed as pK_a values) are 11.0, 9.9, 6.3, 5.5 and 2.9,[34] The third and fourth protonation steps occur at the pendent amines as shown by crystallography.[35] Using this information, one of the two primary amines is fully protonated at pH 5.5, and hence protected from reaction with an aldehyde. Thus pH control then provides a high yielding route toward monosubstituted products (HL^{10}), as desired here, while raising the pH above 5.5 generates a greater proportion of disubstituted product (H$_2$L^4). Reduction of the imine intermediate can be achieved selectively with sodium cyanoborohydride, which reacts only slowly with aldehydes at this pH.[36] Reaction conditions were optimised to utilise a three-fold excess of reducing agent, increasing the rate of secondary amine formation in preference to intramolecular attack upon the imine by an adjacent macrocyclic amine. This latter unwanted reaction leads to formation of a five membered imidazolidine ring.[37]

The ligand HL^{10} will inevitably exist in solution as a zwitterion so extraction of the ligand from the crude reaction mixture was not possible. Instead, purification of L^{10} as its Co^{III} complex was our goal and this was relatively straightforward using cation exchange chromatography. Complexes of L^{10} could be easily separated from known complexes of the parent ligand L^1.[2,26] The presence of cyanide in the reaction mixture results from decomposition of cyanoborohydride and this highly competitive ligand is scavenged by the cobalt ion resulting in both mono- and dicyano complexes. Formation of these cyano complexes can be reduced to trace amounts by acidification of the reaction mixture and purging with air (to drive off HCN) prior to complexation with cobalt. This enabled the more synthetically useful hydroxo and aqua complexes [CoL^{10}(OH)]$^+$ and [CoL^{10}(OH$_2$)]$^{2+}$ to be obtained as precursors to dinuclear cyano-bridged species (see below).

Synthesis of the dinuclear complex [CoL^{10}-μ-NC-Fe(CN)$_5$]$^{2-}$ was also facile and followed well established synthetic methods[38–40] that benefit (thermodynamically and kinetically) from the electrostatic attraction, ion pair formation and outer sphere electron transfer between the reactants ([CoL^{10}(OH$_2$)]$^{2+}$ and [Fe(CN)$_6$]$^{4-}$), which generates a substitution labile Co^{II} complex as an intermediate which is attacked by ferricyanide. The cyano complex [CoL^{10}(CN)]$^+$ failed to react with [Fe(CN)$_6$]$^{4-}$ at pH 8. This is most likely related to the cathodically shifted Co$^{III/II}$ redox potential relative to the aqua complex, which is too negative to be reduced by ferrocyanide and the lower charge which diminishes the electrostatic contribution to the driving force of the reaction. Reactions leading to cyano-bridged complexes of this type may proceed by direct substitution on the Co^{III} centre by ferricyanide (without reduction) but require good leaving groups such as chloro or aqua in the site of substitution on the Co^{III} precursor. In this case the cyano ligand is too tightly bound to Co^{III} and cannot be displaced by the ferrocyanide anion. Although [CoL^{10}(CN)]$^+$ is an unsuitable precursor to [CoL^{10}-μ-NC-Fe(CN)$_5$]$^{2-}$, it offers a potential route to the linkage isomer [CoL^{10}-μ-CN-Fe(CN)$_5$]$^{2-}$. We are currently exploring this possibility with Co^{III} complexes of L^2 in reaction with pentacyanoferrate(II) precursors.

Table 1 Solvatochromism of MMCT Transition of [CoL^{10}-μ-NC-Fe(CN)$_5$]$^{2-}$

Solvent	$\tilde{\nu}_{MMCT}$/cm^{-1}	Colour	AN[46,47]
H$_2$O	19720	Maroon–red	54.8
MeOH	18110	Purple	41.3
Ethylene glycol	17990	Purple	42.8
DMSO	16430	Blue	19.3

Crystal structures

The X-ray crystal structure of [Co(HL^{10})(CN)](ClO$_4$)$_2$·H$_2$O reveals all molecules on general positions with one perchlorate anion rotationally disordered about a Cl–O axis. A view of the complex cation is shown in Fig. 1 where pentadentate coordination of the macrocycle is apparent with the substituted exocyclic amine remaining uncoordinated. The six-coordinate geometry of the complex is completed by a C-bound cyano ligand *trans* to the pendent amine. The Co–N bond lengths (Table 1) are typical of pentadentate coordinated Co^{III} complexes of L^1 and L^2 and their derivatives.[3,7,26,38,41,42] The cyano ligand exhibits a significant *trans* influence on the Co–N5 bond length, which is notably longer than the other four Co–N bonds. This has been seen in other related pendent amino-macrocyclic cyanocobalt(III) complexes of L^1 and L^2.[7,26,42] The hydroxyl proton attached to O2 was located from difference maps and the disparity in the C21–O1 and C21–O2 bond lengths supports this assignment.

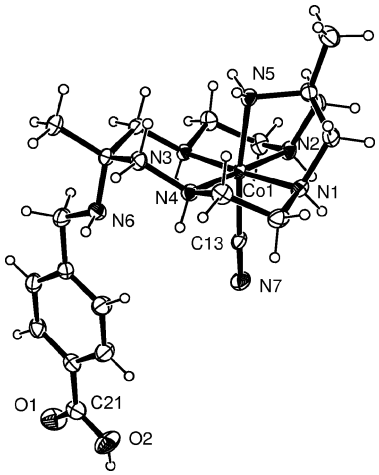

Fig. 1 View of [Co(HL^{10})(CN)]$^{2+}$ (30% ellipsoids). Selected bond lengths (Å) Co(1)–C(13) 1.893(3), Co(1)–N(1) 1.957(3), Co(1)–N(2) 1.947(3), Co(1)–N(3) 1.958(2), Co(1)–N(4) 1.958(3), Co(1)–N(5) 1.979(3), C(21)–O(1) 1.203(5), C(21)–O(2) 1.327(5).

The secondary amine N-donors adopt the *trans*-I (*RSRS*) configuration where all H-atoms lie on the same side of the macrocycle. In this conformation, H-bonding between the non-coordinated amine (N6) and the adjacent secondary amine H-atoms is enabled, although these interactions are relatively weak;

a consequence of constraints of the chelate ring to which the pendent amine is attached. There are stronger intermolecular H-bonds involving the complex, perchlorate anions and water molecule.

The crystal structure of $[CoL^{10}(OH)]ClO_4 \cdot 5H_2O$ (Fig. 2) was also determined and in this case the carboxylate form of the macrocyclic ligand is evident. Of note is an intramolecular H-bond between the hydroxo ligand and the non-coordinated amine (O1–H $\cdots$ N6). This draws the pendent amine ~0.5 Å closer to the metal; N6 $\cdots$ O1 3.21 Å in the hydroxo complex *cf.* N6 $\cdots$ C13 3.73 Å in $[Co(HL^{10})(CN)](ClO_4)_2$. The configuration of the secondary amine donors is identical to that seen in the cyano analogue. In contrast to $[Co(HL^{10})(CN)](ClO_4)_2 \cdot H_2O$, in the absence of a *trans* influence from the hydroxo ligand the Co–N5 bond length is similar to the other Co–N coordinate bonds.

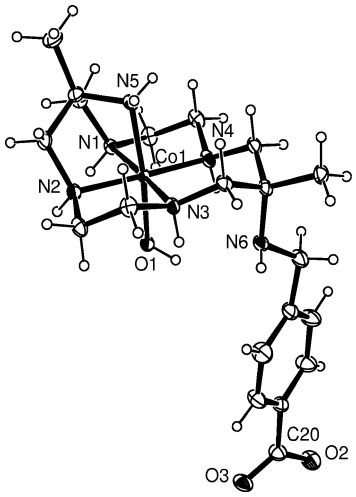

Fig. 2 View of $[CoL^{10}(OH)]^+$ (30% ellipsoids). Selected bond lengths (Å) Co(1)–O(1) 1.910(3), Co(1)–N(1) 1.949(4), Co(1)–N(2) 1.950(4), Co(1)–N(3) 1.943(4), Co(1)–N(4) 1.954(4), Co(1)–N(5) 1.967(4), C(20)–O(2) 1.265(7), C(20)–O(3) 1.257(7).

Electronic spectroscopy and solvatochromism

The mononuclear cobalt(III) complexes were found to exhibit electronic maxima corresponding to previously characterised cyano and hydroxo pentaamine cobalt(III) complexes.[7] The electronic spectrum of $[CoL^{10}$-μ-NC-$Fe(CN)_5]^{2-}$ exhibited a number of features characteristic of similar mixed valence complexes we have studied.[38–40,43] The most prominent feature is the metal-to-metal charge transfer (MMCT) transition (*ca.* 510 nm, $Fe^{II} \rightarrow Co^{III}$) in addition to d–d transitions characteristic of the individual ferrocyanide ($^1T_{1g} \leftarrow {}^1A_{1g}$ (O_h) *ca.* 325 nm) and $Co^{III}N_6$ ($^1T_{1g} \leftarrow {}^1A_{1g}$ (O_h) *ca.* 440 nm) chromophores. The higher energy Co^{III} transition ($^1T_{2g} \leftarrow {}^1A_{1g}$ (O_h)) was obscured by the greater intensity iron(II) ($^1T_{1g} \leftarrow {}^1A_{1g}$ (O_h)) band.

Oxidation of the red $[Co^{III}L^{10}$-μ-NC-$Fe^{II}(CN)_5]^{2-}$ in aqueous solution with potassium peroxydisulfate results in the yellow $Co^{III}(HL^{10})$-μ-NC-$Fe^{III}(CN)_5$ complex. Mechanistic studies of this type of oxidation reaction have been reported elsewhere.[44,45] In our studies with dinuclear complexes of this type,[38,40,45] we have observed that the fully oxidised dinuclear complexes are poorly soluble in water due to their charge neutrality and readily isolated as a consequence. The Co^{III}–$Fe^{II} \rightarrow Co^{III}$–$Fe^{III}$ oxidation reaction takes place over a period of minutes to hours depending on how much $S_2O_8^{2-}$ is added, and thus may be conveniently monitored spectrophotometrically. Observed spectral changes include the loss of the MMCT transition and the emergence of a typical ferricyanide absorption band (*ca.* 400–420 nm) coupled with loss of the MMCT transition at 510 nm that is characteristic of this family of cyano bridged compounds.[38,40,43]

All previously isolated cyano-bridged dinuclear complexes from this family have been virtually insoluble in any pure solvent other than water.[38,40] In this case, the aromatic substituent on $[Co^{III}(HL^{10})$-μ-NC-$Fe^{II}(CN)_5]^-$ renders it partially soluble in hydroxylic organic solvents such as ethylene glycol or methanol and also the aprotic solvent DMSO. The electronic spectra measured in these solvents are shown in Fig. 3, where pronounced solvatochromism of the MMCT transition is seen. The energy of the MMCT transition of $[CoL^{10}$-μ-NC-$Fe(CN)_5]^{2-}$ decreases with decreasing solvent polarity (Table 1) from *ca.* 510 nm (red in water) → *ca.* 600 nm (blue in DMSO). As the complex was only partially soluble in MeOH and DMSO, saturated solutions were prepared then filtered so all of the absorbances have been normalised in the absence of known concentrations. The energies of the localised d–d transitions at ~440 (Co) and 325 nm (Fe) were insensitive to solvent.

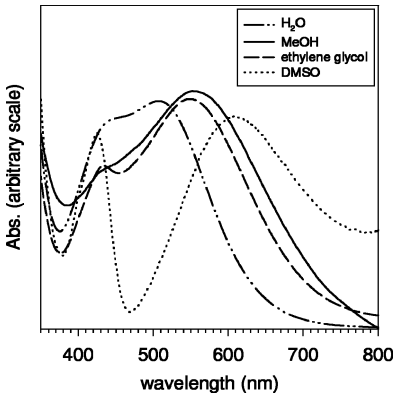

Fig. 3 Solvatochromism of the MMCT transition of $[Co^{III}(HL^{10})$-μ-NC-$Fe^{II}(CN)_5]^-$.

Interactions between the solvent and solute are defined based on the electron donating or accepting ability of the solvent, and this has been quantified by Guttmann in terms of solvent donor number (DN) and acceptor number (AN). Solvatochromism of $[CoL^{10}$-μ-NC-$Fe(CN)_5]^{2-}$ is complicated by the fact that there are terminal cyano ligands as electron donors and amine protons as electron acceptors present.[48,49] Although there are only four data pairs, the energy of the MMCT transition is proportional to the solvent acceptor and follow the empirical formula $\bar{\nu}_{MMCT} = A + B \cdot AN$,[49] giving 14556 cm^{-1} and $B = 89$ cm^{-1} AN^{-1} (correlation coefficient 0.95). The value of B reflects the polarity and asymmetry of the molecule and this magnitude is typical of Robin–Day Class II mixed valence complexes.[48,49] Positive solvatochromism leads to an increase in the energy of the MMCT transition with an increase in the electron acceptor properties of the solvent.[46] In simple terms, the Lewis basicity of the terminal cyano N-atoms will be greater in the ground state (Fe^{II}–CN) than the excited state (Fe^{III}–CN), due to the inductive effect of the metal. Therefore, solvents with a greater capacity for electron acceptance (from the terminal cyano ligands) stabilise the ground state (Co^{III}–Fe^{II}) more than the excited state (Co^{II}–Fe^{III}). By contrast, the poor electron acceptor DMSO cannot solvate the terminal cyano ligands in either oxidation state.

Electron donating solvents will interact with the amine protons and similarly this effect will be more significant for the Co^{III}–NH groups than Co^{II}–NH due to greater polarisation of the N–H bonds in the ground state. However, all of the solvents examined here have rather similar DN values (all bear at least one O-atom donor) so these effects are less important across the present series.

Electrochemistry

Cyclic voltammograms were obtained for mononuclear and dinuclear complexes of L^{10}. The complex $[CoL^{10}(OH_2)]^{2+}$ (the conjugate acid of the structurally characterised $[CoL^{10}(OH)]^+$) was examined at pH 7 on a hanging mercury drop electrode and exhibited a reversible $Co^{III/II}$ redox potential at −587 mV

vs. Ag/AgCl. The hydroxo analogue $[CoL^{10}(OH)]^{+}$ (dominant at pH 12) displayed a redox potential of −707 mV *vs.* Ag/AgCl, a cathodic shift that is consistent with the electrostatic effect of deprotonation of the aqua ligand.

The dinuclear complex $[CoL^{10}$-μ-NC-$Fe(CN)_5]^{2-}$ exhibits waves corresponding to the $Co^{III/II}$ and $Fe^{III/I}$ redox couples (Fig. 4). A totally reversible $Fe^{III/II}$ couple at 411 mV *vs.* Ag/AgCl was identified using a glassy carbon working electrode which is similar to that found previously with similar Co^{III}–Fe^{II} complexes from this family.[38,40] These values are *ca.* 200 mV more positive than $[Fe(CN)_6]^{3-/4-}$ illustrating the electrostatic influence of the positively charged $\{Co^{III}L^{10}\}^{2+}$ moiety. Quasi-reversible $Co^{III/II}$ waves were observed on glassy carbon. This voltammetric behaviour appears to be due to both sluggish electron transfer and lability of the fully reduced Co^{II}–Fe^{II} complex. Evidence for the latter comes from the emergence of new $Fe^{III/II}$ waves on successive cycles that are consistent with the formation (within the diffusion layer) of equal amounts of the trinuclear derivative $[CoL^{10}$-μ-NC-$Fe(CN)_4$-μ-CN-$CoL^{10}]$ ($Fe^{III/II}$ 600 mV) and free ferrocyanide ($Fe^{III/II}$ 230 mV), as reported before for other members of this series.[38,40] These additional $Fe^{III/II}$ waves are absent in the initial anodic sweep thus reduction of the Co^{III} centre is necessary for this rearrangement to take place. The $Co^{III/II}$ redox potential was found at −685 mV, which is *ca.* 150 mV more negative than that seen in $[CoL^{10}(OH_2)]^{2+}$ and attributable to the influence of the coordinated negatively charged ferrocyanide group.

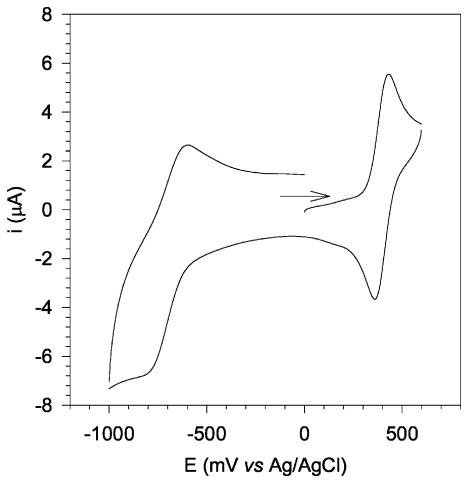

Fig. 4 Cyclic voltammogram of $[CoL^{10}$-μ-NC-$Fe(CN)_5]^{2-}$ (aqueous solution, sweep rate 100 mV s^{-1}). Arrow shows initial direction of sweep.

Chemisorption to titania

The main objective of this work was to develop carboxylic acid functionalised macrocyclic complexes that could be bound (irreversibly) to optically transparent conducting surfaces. As proof of concept, we chose the dinuclear complex $[Co(HL^{10})$-μ-NC-$Fe(CN)_5]^{-}$ as the adsorbate. This compound, like other mixed valence complexes from its family, exhibits a prominent visible MMCT transition that is sensitive to redox reactions at either metal centre. Also, the electrochemistry of the ferri/ferrocyanide moiety is well behaved and these two properties may be examined simultaneously in a spectroelectrochemical experiment to examine various properties of the film including electrochemical communication between the complex and the electrode, optical switching time and the concentration of adsorbate within the film.

The coupling between a carboxylic acid and titania requires the TiO_2 surface to bear a high concentration of hydroxyl groups that enable the elimination of water upon formation of the Ti–O–COR bond. The isoelectric point of titania is in the range pH 5.5 to 6.5 so on this basis, acidic aqueous solutions are required for successful chemisorption of carboxylic acids to titania. Successful chemisorption of $[CoL^{10}$-μ-NC-$Fe(CN)_5]^{2-}$ was achieved from acidified aqueous solution (pH 3.5) and a 1 : 1 mixture of MeOH : EtOH. Previous studies on the binding of carboxylic acids to titania have utilised the protonated (acid) form of the molecule.[15,50,51] There was no apparent leaching of complex from either film soaked in MeOH, but soaking the films in water at pH 7 led to significant loss of complex as a result of hydroxide ion attack on the Ti–O(carboxylate) bonds. More detailed kinetic studies of this process and an optimal method for chemisorption and stabilisation of the adsorbed complex are underway.

X-ray photoelectron spectroscopy was utilised to characterise titania films that included the dinuclear complex $[CoL^{10}$-μ-NC-$Fe(CN)_5]^{2-}$ chemisorbed using the aqueous method (i) in the Experimental section. The spectrum of $[CoL^{10}$-μ-NC-$Fe(CN)_5]^{2-}$ bound to titania revealed a number of elements, which were charge corrected to titanium(IV) $2p^{3/2}$ (TiO_2, 458.6 eV) and rounded to the nearest electron volt.[52] Observed peaks include: cobalt(III) 797 eV ($2p^{1/2}$), 782 eV ($2p^{3/2}$); iron(II) 721 eV ($2p^{1/2}$), 708 eV ($2p^{3/2}$); oxygen 530 eV (1s); titanium(IV) 464 eV ($2p^{1/2}$), 456.8 eV ($2p^{3/2}$); nitrogen 400 eV (1s) and carbon 285 eV (1s).

Chemisorption of $[Co(HL^{10})CN](ClO_4)_2$ onto P25 titania films was unsuccessful when experimental procedures successful for $[Co(HL^{10})$-μ-NC-$Fe(CN)_5]^{-}$ were employed. The film retained no colour and XPS showed no evidence of complex on the surface of the film. Given the similarities between the two complexes, this result suggests that charge is an important factor in facilitating chemisorption of the complex. In other words, the cation $[Co(HL^{10})CN]^{2+}$ will be repelled by the positively charged titania surface (at pH 3.5) whereas the negatively charged $[Co(HL^{10})$-μ-NC-$Fe(CN)_5]^{-}$ complex will be attracted initially and eventually covalently bound.

Spectroelectrochemistry of titania-adsorbed $[CoL^{10}$-μ-NC)$Fe(CN)_5]^{2-}$

Leaching of $[CoL^{10}$-μ-NC)$Fe(CN)_5]^{2-}$ from the titania film was rapid in neutral aqueous solution so electrochemistry of the adsorbed complex was conducted at pH 4 where no leaching of complex was apparent over the duration of the experiment. The $Fe^{III/II}$ couple was observed but the $Co^{III/II}$ wave was obscured by a large cathodic wave that is most probably proton reduction. For technical reasons a silver wire pseudo reference electrode was used in addition to a Pt wire counter electrode so that all electrodes could be contained within a 1 cm spectrophotometer cuvette. Separate experiments conducted in larger electrochemical cells (without the need for simultaneous optical absorbance measurement) enabled the use of an Ag/AgCl reference electrode and the actual potentials shown in Fig. 5 have been corrected accordingly.

Unlike the solution electrochemistry of $[CoL^{10}$-μ-NC-$Fe(CN)_5]^{2-}$ (Fig. 4) the titania-immobilised complex exhibits more than one $Fe^{III/II}$ wave (Fig. 5, left). This electrochemical complexity may be a consequence of various Ti–O–COR linkages (monodentate/bidentate) and/or different conformations of the redox active molecule. Rearrangement to form other oligomeric complexes on the surface cannot be ruled out either. The peak current was found to be proportional to scan rate which is consistent with voltammetric responses of a surface confined molecule.[53] As expected from the bistability of this redox couple (both forms isolated as stable solid compounds) the electrochemistry is totally reversible and the $Fe^{III/II}$ redox potential of the immobilised complex (Fig. 5, left) is essentially the same as that determined in solution (Fig. 4). In concert with voltammetry of the surface confined complex, the spectral changes of the optically transparent working electrode were monitored as a function of time (Fig. 5, right). As mentioned previously, the most obvious spectral changes upon oxidation

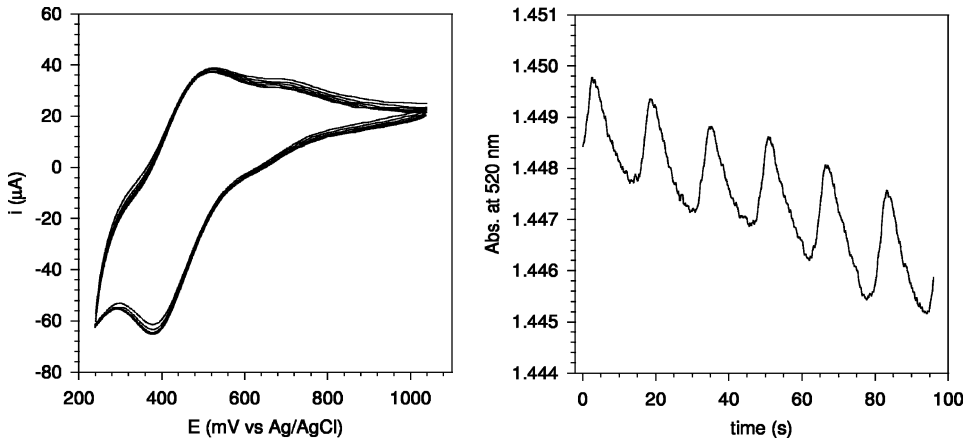

Fig. 5 Left: Cyclic voltammogram of $[CoL^{10}$-μ-NC-$Fe(CN)_5]^{2-}$ chemisorbed on a TiO_2 modified ITO working electrode (6 cycles shown) in aqueous solution (pH 4). Right: Simultaneous absorbance changes of optically transparent working electrode at 520 nm as a function of time (note 16 s periodicity).

will be the loss of the visible MMCT band (*ca.* 520 nm) of the Co^{III}–Fe^{II} complex with a concomitant rise in absorption from the ferrocyanide chromophore (400–420 nm). The cathodic and anodic sweeps were 800 mV which equates to a cycle of 16 s at the sweep rate of 100 mV s^{-1} (Fig. 5, right).

The redox-linked absorbance changes at 520 nm are rapid and not rate limiting at 100 mV s^{-1}. There is a baseline absorbance drift over the 100 s period shown (*ca.* 6 cycles). The baseline absorbance (~1.44 units on the scale shown) is due to the titania film and the changes over the course of the experiment perhaps are related to variations in hydration of the porous titania structure driven by the redox reaction of the complex.

The amount of electroactive complex can be determined directly by integrating the current under the voltammetric curves (Fig. 5, left) with respect to time. This gave a value in the conservative range 100–200 pmol. The greatest uncertainty in this number emerges from an accurate background current subtraction. The optical absorbance changes (*ca.* 0.002) are directly proportional to the amount of electroactive complex. The extinction coefficient of the complex is *ca.* 500 dm^3 mol^{-1} cm^{-1} (5×10^{-2} dm^3 mol^{-1} μm^{-1}) and the titania film thickness (optical path length) is estimated to be *ca.* 20 μm on the basis that (i) the thickness of the tape used in the drag-coating procedure (~25 μm) will be an upper bound[27]) and (ii) there will be some shrinkage upon dehydration of the film. Assuming that the complex is evenly distributed within the film we arrive at a concentration of electroactive complex within the film of *ca.* 2 mmol dm^{-3}. Coupled with the charge calculation above, this leads to an estimation of the volume of the electroactive film of *ca.* 50–100 $\times$ 10^{-9} dm^{-3}.

A similar experiment was conducted on the film prepared in non-aqueous solution (nonaqueous method (ii) in Experimental section) using MeCN as the solvent for electrochemistry. Under these conditions variations due to hydrolysis of the Ti–OCOR linkages and the level of hydration of the film during the course of the experiment are eliminated. A silver wire pseudo reference was again used and in this case the potentials have not been calibrated. The most important difference between this experiment (Fig. 6) and that conducted in water (Fig. 5, left) is the greater homogeneity of the $Fe^{III/II}$ voltammogram. A single response is seen in each sweep although there is a slight cathodic shift in the average peak potential over successive cycles. The baseline drift of the absorbance change over the duration of this experiment (not shown) is small and the amplitude of the change was *ca.* 0.003 absorbance units. Similar charge calculations as presented above lead to *ca.* 300 pm of electroactive complex. Given the approximations made this is not considered significantly different to the calculations made with the films examined in water.

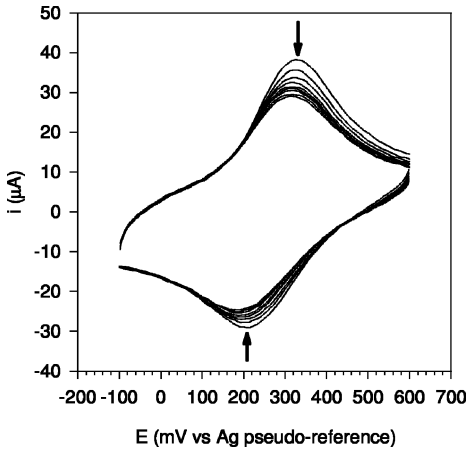

Fig. 6 Cyclic voltammogram of $[Co(L^{10}$-μ-NC-$Fe(CN)_5]^{2-}$ chemisorbed on a TiO_2 modified ITO working electrode in MeCN (Ag wire pseudo reference, 9 cycles shown).

Conclusions

The 4-carboxyphenyl-appended cyclam derivative HL^{10} has been synthesised and it has been shown to be an effective pentadentate ligand for Co^{III} where the substituted amine remains free from the metal. The cyano-bridged complex $[CoL^{10}$-μ-NC-$Fe(CN)_5]^{2-}$ was prepared and chemisorbed on titania-coated ITO conducting glass. In this form, the adsorbed complex was electrochemically active and cyclic voltammetry of the modified ITO working electrode was performed with simultaneous optical spectroscopy. This experiment demonstrated that electrochemical switching was rapid. Although the magnitudes of the absorbance changes in these experiments are too small to be of practical use in electrochromic devices, other more intensely coloured dyes comprising a coordinated macrocyclic ligand such as HL^{10} may be envisaged that would lead to significant absorbance changes upon oxidation or reduction. This is work that is currently underway in our group.

References

1 P. Comba, N. F. Curtis, G. A. Lawrance, A. M. Sargeson, B. W. Skelton and A. H. White, *Inorg. Chem.*, 1986, **25**, 4260–4267.
2 P. V. Bernhardt, G. A. Lawrance and T. W. Hambley, *J. Chem. Soc., Dalton Trans.*, 1989, 1059–1065.
3 G. A. Lawrance, T. M. Manning, M. Maeder, M. Martinez, M. A. O'Leary, W. C. Patalinghug, B. W. Skelton and A. H. White, *J. Chem. Soc., Dalton Trans.*, 1992, 1635–1641.
4 G. A. Lawrance, M. Rossignoli, B. W. Skelton and A. H. White, *Aust. J. Chem.*, 1987, **40**, 1441–1449.

5 P. D. Beer and P. V. Bernhardt, *J. Chem. Soc., Dalton Trans.*, 2001, 1428–1431.
6 P. V. Bernhardt, B. M. Flanagan and M. J. Riley, *J. Chem. Soc., Dalton Trans.*, 1999, 3579–3584.
7 P. V. Bernhardt and E. J. Hayes, *Inorg. Chem.*, 2002, **41**, 2892–2902.
8 P. V. Bernhardt and P. C. Sharpe, *Inorg. Chem.*, 2000, **39**, 4994–4995.
9 P. V. Bernhardt and P. C. Sharpe, *Inorg. Chem.*, 2000, **39**, 4123–4129.
10 P. V. Bernhardt and N. L. Creevey, *Dalton Trans.*, 2004, 914–920.
11 U. Diebold, *Appl. Phys. A*, 2003, **76**, 681–687.
12 H. Frei, D. J. Fitzmaurice and M. Grätzel, *Langmuir*, 1990, **6**, 198–206.
13 G. Redmond, D. Fitzmaurice and M. Grätzel, *J. Phys. Chem.*, 1993, **97**, 6951–6954.
14 G. Y. Popova, T. V. Andrushkevich, Y. A. Chesalov and E. S. Stoyanov, *Kinet. Catal.*, 2000, **41**, 805–811.
15 W. J. E. Beek and R. A. J. Janssen, *Adv. Funct. Mater.*, 2002, **12**, 519–525.
16 M. Grätzel, *Nature*, 2001, **414**, 338–344.
17 M. Biancardo, P. F. H. Schwab, R. Argazzi and C. A. Bignozzi, *Inorg. Chem.*, 2003, **42**, 3966–3968.
18 R. Argazzi, N. Y. Murakami Iha, H. Zabri, F. Odobel and C. A. Bignozzi, *Coord. Chem. Rev.*, 2004, **248**, 1299–1316.
19 I. Gillaizeau-Gauthier, F. Odobel, M. Alebbi, R. Argazzi, E. Costa, C. A. Bignozzi, P. Qu and G. J. Meyer, *Inorg. Chem.*, 2001, **40**, 6073–6079.
20 F. Campus, P. Bonhote, M. Grätzel, S. Heinen and L. Walder, *Sol. Energy Mater. Sol. Cells*, 1999, **56**, 281–297.
21 R. Cinnsealach, G. Boschloo, S. N. Rao and D. Fitzmaurice, *Sol. Energy Mater. Sol. Cells*, 1998, **55**, 215–223.
22 R. Cinnsealach, G. Boschloo, S. N. Rao and D. Fitzmaurice, *Sol. Energy Mater. Sol. Cells*, 1999, **57**, 107–125.
23 D. Cummins, G. Boschloo, M. Ryan, D. Corr, S. N. Rao and D. Fitzmaurice, *J. Phys. Chem. B*, 2000, **104**, 11449–11459.
24 P. V. Bernhardt, P. Comba, T. W. Hambley, G. A. Lawrance and K. Varnagy, *J. Chem. Soc., Dalton Trans.*, 1992, 355–359.
25 H. F. Bauer and W. C. Drinkard, *J. Am. Chem. Soc.*, 1960, **82**, 5031–5032.
26 P. V. Bernhardt and N. L. Kilah, *Acta Crystallogr., Sect. C*, 2005, **61**, m245–m249.
27 G. P. Smestad and M. Grätzel, *J. Chem. Educ.*, 1998, **75**, 752–756.
28 S. Ito, T. Kitamura, Y. Wada and S. Yanagida, *Sol. Energy Mater. Sol. Cells*, 2003, **76**, 3–13.
29 A. C. T. North, D. C. Phillips and F. S. Mathews, *Acta Crystallogr., Sect. A*, 1968, **A24**, 351.
30 L. J. Farrugia, *J. Appl. Crystallogr.*, 1999, **32**, 837.
31 G. M. Sheldrick, *SHELXL-97: Program for Crystal Structure Refinement*, University of Göttingen, Göttingen, 1997.
32 L. J. Farrugia, *J. Appl. Crystallogr.*, 1997, **30**, 565.
33 P. V. Bernhardt, E. G. Moore and M. J. Riley, *Inorg. Chem.*, 2002, **41**, 3025–3031.
34 P. V. Bernhardt, G. A. Lawrance, M. Maeder, M. Rossignoli and T. W. Hambley, *J. Chem. Soc., Dalton Trans.*, 1991, 1167–1170.
35 P. V. Bernhardt, T. W. Hambley and G. A. Lawrance, *Aust. J. Chem.*, 1990, **43**, 699–706.
36 R. F. Borch, M. D. Bernstein and H. D. Durst, *J. Am. Chem. Soc.*, 1971, **93**, 2897–2904.
37 P. V. Bernhardt and P. C. Sharpe, *Inorg. Chem.*, 2000, **39**, 2020–2025.
38 P. V. Bernhardt, B. P. Macpherson and M. Martinez, *Inorg. Chem.*, 2000, **39**, 5203–5208.
39 P. V. Bernhardt and M. Martinez, *Inorg. Chem.*, 1999, **38**, 424–425.
40 P. V. Bernhardt, B. P. Macpherson and M. Martinez, *J. Chem. Soc., Dalton Trans.*, 2002, 1435–1441.
41 P. V. Bernhardt and B. P. Macpherson, *Acta Crystallogr., Sect. C*, 2003, **C59**, m467–m470.
42 P. V. Bernhardt and B. P. Macpherson, *Acta Crystallogr., Sect. C*, 2003, **C59**, m533–m536.
43 P. V. Bernhardt, F. Bozoglian, B. P. Macpherson and M. Martinez, *Dalton Trans.*, 2004, 2582–2587.
44 P. V. Bernhardt, F. Bozoglian, B. P. Macpherson, M. Martinez, G. Gonzalez and B. Sienra, *Eur. J. Inorg. Chem.*, 2003, 2512–2518.
45 P. V. Bernhardt, F. Bozoglian, B. P. Macpherson, M. Martinez, A. E. Merbach, G. Gonzalez and B. Sienra, *Inorg. Chem.*, 2004, **43**, 7187–7195.
46 W. Linert, Y. Fukuda and A. Camard, *Coord. Chem. Rev.*, 2001, **218**, 113–152.
47 H. Tanida, H. Sakane and I. Watanabe, *J. Chem. Soc., Dalton Trans.*, 1994, 2321–2326.
48 W. M. Laidlaw and R. G. Denning, *Inorg. Chim. Acta*, 1996, **248**, 51–58.
49 M. Glockle, N. E. Katz, M. Ketterle and W. Kaim, *Inorg. Chim. Acta*, 2002, **336**, 55–60.
50 G. J. Meyer, *J. Chem. Educ.*, 1997, **74**, 652–656.
51 R. E. Tanner, Y. Liang and E. I. Altman, *Surf. Sci.*, 2002, **506**, 251–271.
52 J. L. G. Fierro, L. A. Arrua, J. M. L. Nieto and G. Kremenic, *Appl. Catal.*, 1988, **37**, 323–338.
53 A. J. Bard and L. R. Faulkner, *Electrochemical Methods: Fundamentals and Applications*, John Wiley, 2001.